https://doi.org/10.5194/egusphere-2026-973
Preprint. Discussion started: 4 March 2026

European runoff drought event types: From historical classification to projected future changes

Sadaf Nasreen[1], Oldrich Rakovec[1], Rohini Kumar[2], Manuela I. Brunner[4,5,6], Ujjwal Singh[1], Petr Maca[1], Yannis Markonis[1], and Martin Hanel[1,3]

[1]Faculty of Environmental Sciences, Czech University of Life Sciences Prague, Praha-Suchdol 16500, Czech Republic
[2]UFZ-Helmholtz Centre for Environmental Research, Leipzig 04318, Germany
[3]T.G. Masaryk Water Research Institute, Podbabska 30, Praha 6, 16000, Czech Republic
[4]WSL Institute for Snow and Avalanche Research SLF, Davos Dorf, Switzerland
[5]Institute for Atmospheric and Climate Science, ETH Zurich, Zurich, Switzerland
[6]Climate Change, Extremes and Natural Hazards in Alpine Regions Research Center CERC, Davos Dorf, Switzerland

Correspondence: Sadaf Nasreen (nasreen@fzp.czu.cz)

Abstract. European drought events have intensified in recent decades, raising concerns about water resources, agriculture, and ecosystem health. Most existing continental-scale drought assessments provide limited attribution of drought changes to the processes that generate runoff drought, which constrains understanding of how these processes will evolve in a warming climate. In this study, we provide the first continental-scale assessment of future changes in runoff drought generation processes across Europe, focusing on rainfall deficit, rain-to-snow and wet-to-dry season transitions, and snow-related processes. We used a continental-scale hydrological model in combination with observed meteorological data and climate simulations (GCMs) under a middle-of-the-road emission scenario (i.e., RCP4.5, ≈2°C global warming by 2100). Unlike widely used aggregated drought index-based studies, our mechanism-specific classification approach distinguishes the physical drivers of drought events by classifying runoff droughts into seven event types based on their severity, duration, and frequency and leverages spatial clustering analysis (Getis–Ord G_i^* method) to assess the climate responses. Our analysis reveals considerable regional differences in drought mechanisms and their responses. Historical observations (1971–2000) highlight that Mediterranean Europe experiences the most severe drought conditions, dominated by rainfall deficit processes and wet-to-dry season transitions, with deficits exceeding (> 4 mm day^{-1}), prolonged durations (> 165 days), and high event frequencies. Future projections (2070–2099) indicate further drought intensification in the Mediterranean driven by increasing rainfall deficit and wet-to-dry transition events, with runoff deficit increases by 2–6 mm day^{-1} and duration extensions exceeding 200 days, while Northern and Western-Central Europe show predominantly decreasing drought severity due to declining cold-snow season droughts under warming conditions. Importantly, drought related to temperature-driven processes, especially those triggered by rain-to-snow transitions, exhibit the most pronounced projected changes. These findings demonstrate that different drought mechanisms respond distinctly to climate forcing. By attributing projected drought changes to specific generation processes, our results enable region-specific interpretation of drought hazard, which is crucial for effective water-resources planning across Europe.

https://doi.org/10.5194/egusphere-2026-973
Preprint. Discussion started: 4 March 2026

Plain Language Summary

Droughts pose significant challenges to European water resources and agriculture; however, we do not yet fully understand how different types of drought processes will evolve as the climate warms. We study seven distinct drought mechanisms across Europe using historical data (1971–2000) and climate projections (2070–2099), revealing that drought changes vary dramatically by region. The Mediterranean will experience more severe drought events with longer durations, while Northern and Western-Central Europe will generally see improvements. Temperature-driven processes, such as rain-to-snow transitions (rainfall deficits that continue into the snow season once temperatures fall below 0 °C), show the strongest responses to warming. This process-based approach provides new insights to design targeted regional adaptation strategies and can be applied globally to understand how different drought mechanisms respond to climate change.

1 Introduction

Drought is a complex hydroclimatic phenomenon with significant ecological, economic, and societal impacts across Europe (Stahl et al., 2016; Spinoni et al., 2018). Recent major events, including the 2003 heatwave–drought (Ciais et al., 2005), the 2010–2012 drought in southern Europe (Spinoni et al., 2015), and the unprecedented 2018–2019 drought across central and northern Europe (Buras et al., 2020; Hari et al., 2020), highlight the continent's growing drought affectedness, with widespread impacts on agriculture, forestry, water supply, and the energy sector (Stahl et al., 2016). These events show pronounced spatial heterogeneity in drought responses, indicating that distinct hydroclimatic mechanisms governing drought development respond differently to climate forcing across regional contexts. As global warming is projected to alter drought characteristics, most notably their frequency, intensity, and duration (Masson-Delmotte et al., 2021), understanding how specific drought mechanisms respond to changes in climate forcing has become a critical challenge. However, these projected changes are regionally heterogeneous due to differences in climate dynamics, land–surface interactions, and hydrological processes (Gudmundsson and Seneviratne, 2016; Samaniego et al., 2018).

Classification of drought events by their underlying physical processes offers a framework to assess how climate change affects drought-generating mechanisms (Van Loon and Van Lanen, 2012; Brunner et al., 2021). Events can be grouped into those driven by precipitation deficits (rainfall deficit), seasonal regime shifts (wet-to-dry or rain-to-snow transitions), and snow-related processes (warm snow, cold snow, snowmelt). Such categorization facilitates attribution of hydrological deficits to specific drivers (Brunner et al., 2021). Each drought event type also shows distinct spatiotemporal characteristics and responds differently to climatic forcing (Apurv et al., 2017), providing a direct link between drought processes and the magnitude, timing, and impacts of hydrological changes.

Typology-based drought analyses remain relatively rarely applied and are typically restricted to regional or catchment scales (Van Loon and Van Lanen, 2012; Brunner et al., 2021; Barker et al., 2016; Haslinger et al., 2014), or focus on specific drought event types (Hanel et al., 2018; Marx et al., 2018; Markonis et al., 2021). Most critically, climate model evaluations rarely rely on such typological frameworks to understand changes in drought generation processes, limiting mechanistic understanding of drought evolution under climate change.

https://doi.org/10.5194/egusphere-2026-973
Preprint. Discussion started: 4 March 2026

As a consequence, it remains largely unknown how different drought generation processes will change in a future climate at the continental scale. This knowledge gap constrains our ability to anticipate the evolution of mechanism-specific drought risks in a warming Europe. In this study, we address this gap by presenting the first European-scale assessment of projected changes in drought generation processes. Specifically, we examine how distinct mechanisms – rainfall deficits, rain-to-snow (rainfall deficits that continue into the snow season once temperatures fall below 0 °C), and wet-to-dry transitions (wet-season precipitation deficits that persist into the dry/high-evaporative-demand season), and snow-related processes (cold/warm snow-season and composite types reflecting anomalous snow accumulation and melt conditions) – respond to changes in climate. In contrast to previous continental-scale studies that relied on aggregated drought indices or focused primarily on meteorological and soil-moisture drought metrics, our approach enables a systematic evaluation of mechanism-specific drought responses to climate change. We base our assessment on observation-based historical meteorological data (EOBS v25, 1971–2000), global circulation model (GCM) simulations (ISIMIP2b, historical 1971–2000 and future RCP4.5 2070–2099), and corresponding hydrological simulations from the mesoscale Hydrological Model (mHM; Samaniego et al., 2010; Kumar et al., 2013). We employ the RCP4.5 emission scenario, which represents a moderate pathway in which greenhouse gas emissions peak around mid-century and then decline. This choice offers a balanced perspective between high-emission (RCP8.5) and low-emission (RCP2.6) futures and is suitable for assessing plausible near- to mid-term climate impacts. By focusing on multiple drought characteristics (severity, duration, frequency, seasonality, and spatial patterns), and applying spatial statistical techniques (Getis–Ord G_i^* hotspot (Getis and Ord, 1992) analysis), we provide a robust framework to anticipate the transformation of drought processes under climate change. Our findings offer critical insights to support adaptive water resources management, regional vulnerability assessments, and the development of effective drought management strategies.

2 Data and methods

We apply a multi-step methodology that combines hydrological modelling with process-based drought classification. First, continental-scale runoff and snow dynamics are simulated using the mesoscale Hydrological Model (mHM; Samaniego et al., 2010; Kumar et al., 2013), forced with two meteorological datasets: observation-based climate data (EOBS v25, (Cornes et al., 2018)) and ISIMIP2b climate model simulations under the RCP4.5 scenario (Frieler et al., 2017). Second, drought events are identified with the threshold level method, defined by parameters for minimum duration, minimum inter-event time, and a severity threshold. Third, these events are classified into seven process-based types following existing drought classification approaches (Van Loon and Van Lanen, 2012; Brunner et al., 2021): rainfall deficit, rain-to-snow and wet-to-dry transitions, snow-related processes (warm snow, cold snow, snowmelt), and composite droughts. Fourth, spatial and temporal patterns of drought characteristics (severity, duration, frequency) are analyzed across three European regions. Finally, we identify statistically significant spatial clusters of process-based responses to climate forcing using Getis–Ord G_i^* hotspot analysis (Getis and Ord, 1992) (a local spatial statistic that identifies significant hot spots/cold spots-clusters of unusually high/low values relative to neighboring cells).

https://doi.org/10.5194/egusphere-2026-973
Preprint. Discussion started: 4 March 2026

2.1 Meteorological data

Meteorological data of daily precipitation and temperature were obtained from the gridded EOBS dataset (Cornes et al., 2018), available at a spatial resolution of 0.25° × 0.25°. These data were analysed for the period 1971–2000. The period 1971–2000 was chosen because it aligns with the historical CMIP5 model runs and available EOBS observational data, ensuring consistency for comparison with future projections under the RCP4.5 scenario.

The climate model simulations were obtained from the Inter-Sectoral Impact Model Intercomparison Project Phase 2b (ISIMIP2b; Frieler et al., 2017), which provides bias-corrected daily precipitation and air temperature from CMIP5 GCMs. In ISIMIP2b, bias correction was applied separately for each variable, grid cell, and calendar month using quantile mapping, aligning the full distribution of model outputs with reference observations (Hempel et al., 2013; Lange, 2019). The data were provided at 0.5° × 0.5° resolution. For our analysis, we selected 1971–2000 as the historical baseline and 2070–2099 for projections under the RCP4.5 scenario. Our study relied on five GCMs, listed in Table 1. RCP4.5 represents a moderate warming pathway, with atmospheric CO_2 concentrations reaching about 650 ppm by 2100 and global mean temperature increases of 1.1–2.6°C above pre-industrial levels (Collins et al., 2013).

For computational efficiency, both observed and GCM-simulated data were aggregated to 5-day means (pentad scale). The analysis was carried out across three distinct European regions, based on the AR6 IPCC Working Group I regional classification (Huang et al., 2023): Northern Europe (NEU), comprising Scandinavia and the Baltic region; Western-Central Europe (WCE), encompassing the British Isles and Central Europe; and the Mediterranean (MED), including Southern Europe and the Mediterranean Basin (Fig. 1). Using the AR6 regions is helpful because it groups areas with comparable hydroclimatic drivers (e.g., snow-influenced NEU, transitional WCE, water-limited MED), facilitation the interpretation of mechanism-specific drought changes.

Table 1. Global climate models (GCMs) used in this study.

HadGEM2-ES	Met Office Hadley Centre
IPSL-CM5A-LR	Institut Pierre-Simon Laplace
MIROC-ESM-CHEM	Japan Agency for Marine-Earth Science and Technology (JAMSTEC), National Institute for Environmental Studies (NIES), and Atmosphere and Ocean Research Institute (AORI), The University of Tokyo
GFDL-ESM2M	National Oceanic and Atmospheric Administration (NOAA) Geophysical Fluid Dynamics Laboratory
NorESM1-M	Norwegian Climate Centre

https://doi.org/10.5194/egusphere-2026-973
Preprint. Discussion started: 4 March 2026

2.2 Mesoscale Hydrologic Model

We employed the spatially explicit, physically-based Mesoscale Hydrologic Model (mHM; Samaniego et al., 2010; Kumar et al., 2013) to simulate key hydrological processes, including canopy interception, snow accumulation and melt, infiltration, soil moisture dynamics, percolation, and runoff generation. The model was forced with gridded daily precipitation and temperature data from the meteorological datasets described above (see Section 2.1). Daily potential evapotranspiration was estimated using the Hargreaves–Samani method (Hargreaves and Samani, 1985), which relies on daily mean, minimum, and maximum air temperatures.

In this study, we primarily focused on analysing total runoff (Q) and snow water equivalent (SWE). Runoff in mHM consists of three components: a threshold-driven fast interflow responding to extreme rainfall and snowmelt events; a non-linear, quasi-permanent slow interflow governed by subsurface water storage availability; and baseflow generated from a linear groundwater reservoir (Samaniego et al., 2010). Snow dynamics of snow accumulation and melt, are simulated using a degree-day method with temperature thresholds determining phase partitioning of precipitation between snow and liquid rainfall (Samaniego et al., 2010). The model has been extensively evaluated against various datasets, including streamflow, evapotranspiration, terrestrial water storage anomalies, and soil moisture, across different spatial resolutions and river basins (e.g. Rakovec et al., 2016; Samaniego et al., 2019; Kumar et al., 2020; Boeing et al., 2022; Fatima et al., 2024; Bevacqua et al., 2024). For a comprehensive overview of the mHM model, including its conceptual framework and potential applications, readers are referred to www.ufz.de/mhm. Our additional and drought-focused evaluation with E-OBS forcing (Fig. S1) shows that mHM reproduces low flows well ($< 5\%$), with close agreement in 10th-percentile flows at 0.125° and 0.5° and generally high KGE ($KGE_{\mathrm{day}} \sim 0.6$–$0.9$) for drought conditions across European basins, supporting its use for runoff and snow-related drought analyses in this study.

2.3 Drought event identification and drought characteristics

Drought events were identified following the approach of Yevjevich et al. (1967), which defines drought as a sequence of consecutive periods during which a hydrometeorological variable remains below a predefined threshold. In our study, the following three parameters were considered to identify drought events. See also Figure 1.

Threshold *(τ)*: The threshold below which conditions are classified as drought calculated separately for each pentad to account for seasonal variability (Tallaksen et al., 1997). Typically the threshold is selected as a specific quantile of the hydrometeorological variable. This percentile-based approach ensures that drought identification is relative to local climatological conditions rather than based on absolute values.

Minimum inter-event time *(mit)*: The minimum number of pentads required between consecutive drought events for them to be considered independent. If the period between two droughts is shorter than the *mit* value, the events are merged into a single, extended drought.

Minimum length *(ml)*: The minimum duration, in pentads, for an event to be classified as a drought. Events shorter than the ml value are excluded.

https://doi.org/10.5194/egusphere-2026-973
Preprint. Discussion started: 4 March 2026

To choose optimal parameters, we conducted a detailed sensitivity analysis with thresholds ranging from 0.05–0.25 (step size: 0.05), *mit* from 2–10 (step size: 1), and *ml* from 2–10 (step size: 1). See Supplementary figures (S2, S3) for details. We selected the final parameters directly from the sensitivity ranges shown in Figs. S2–S3 by inspecting, for each variable separately, the ranges of mit, ml, and τ that produced stable event characteristics. The selected parameters are reported in Table 2.

Furthermore, we also estimated drought duration, severity, and the number of drought events per year. Drought duration was defined as the length of the time period between the onset and termination of a drought event, while drought severity was calculated as the cumulative difference between the drought index and its threshold over the duration of the event.

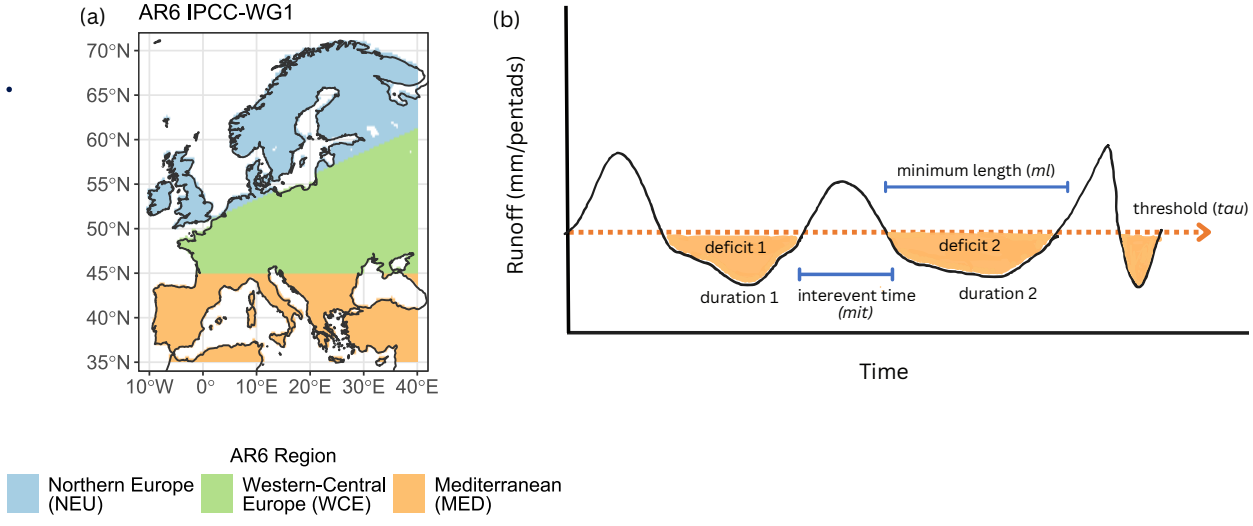

Figure 1. (a) IPCC AR6 Europe regional classification. (b) Schematic of drought characterization and metrics.

Table 2. Selected parameters used for drought event identification.

Variable	Minimum interevent time (mit)	Minimum length (ml)	Threshold (τ)
Precipitation (P)	8	1	0.1
Runoff (Q)	9	8	0.1
Snow water equivalent (SWE)	8	1	0.15

https://doi.org/10.5194/egusphere-2026-973
Preprint. Discussion started: 4 March 2026

2.4 Drought classification

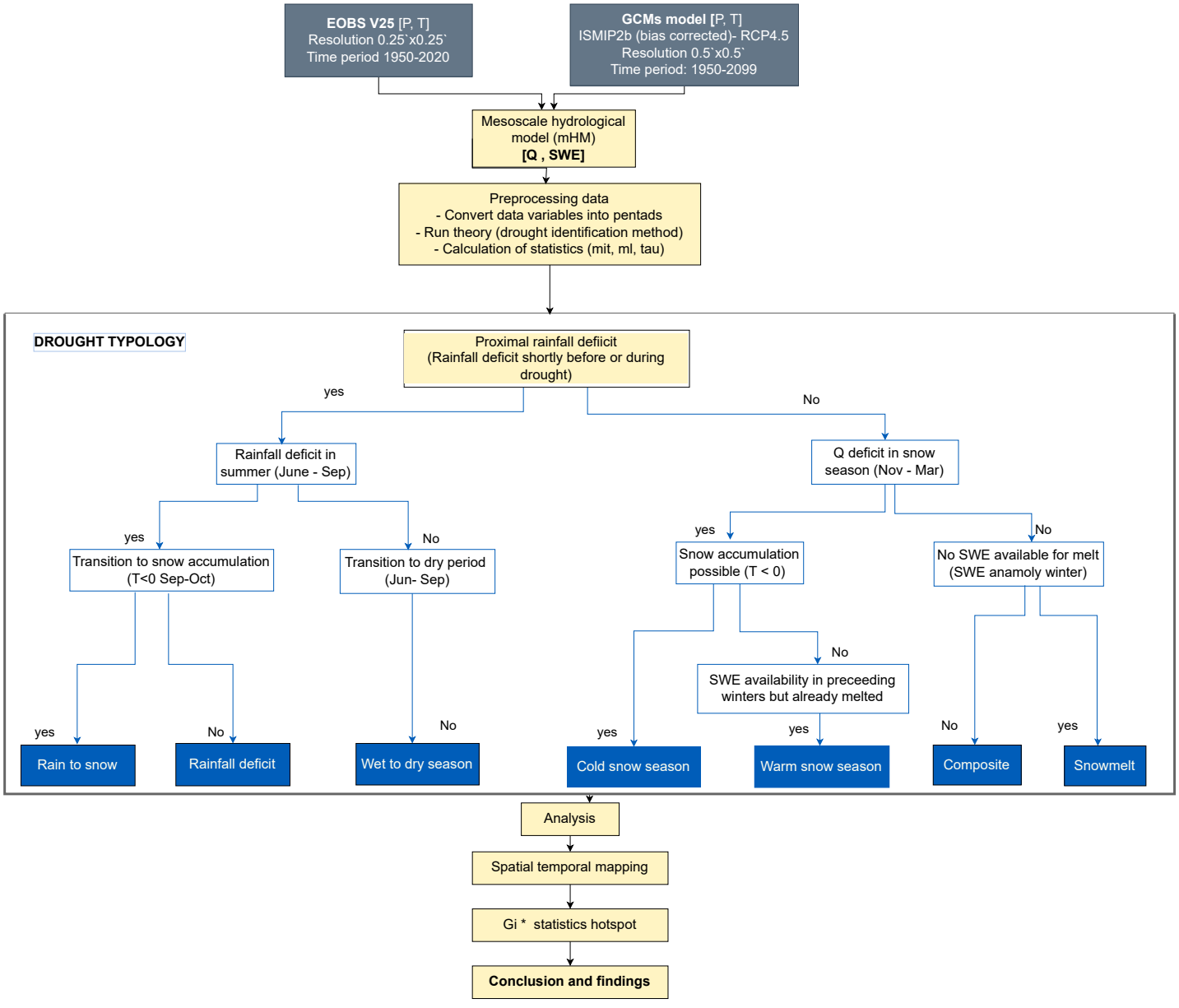

Figure 2. Schematic overview of the data processing and analysis workflow used in this study. The diagram illustrates data sources (EOBS observations and bias-corrected GCM simulations), pre-processing steps (including conversion to pentads and drought identification), and the application of the process-based drought event classification. It also outlines the criteria for classifying droughts by season and hydrological context for the spatio-temporal analyses of drought characteristics.

https://doi.org/10.5194/egusphere-2026-973
Preprint. Discussion started: 4 March 2026

A modified, standardised classification scheme for European runoff droughts was developed based on Brunner et al. (2022). This framework, shown in Fig. 2, categorises hydrological drought events into seven distinct types, considering hydroclimatic drivers such as rainfall deficits, snow availability, and preceding temperature patterns. This approach enables comprehensive drought characterization across thousands of grid cells, achieved through computationally optimised vectorized Boolean operations. We replaced station-based, manual classification with automated, vectorized logic applied to normalized anomalies, enabling robust drought-type mapping across thousands of grid cells. This design preserves mechanistic distinctions while ensuring scalability, consistency, and ensemble robustness for large-scale climate impact assessments.

The classification framework builds upon established drought typology principles, while introducing systematic improvements for large-scale implementation. The drought event typology of (Brunner et al., 2022) builds upon an earlier classification logic proposed by Van Loon and Van Lanen (2012) and Van Loon (2015), which distinguishes between rainfall-influenced types (rain-to-snow season droughts, rainfall deficit droughts, and wet-to-dry season droughts) and snow-driven types (cold snow season droughts, warm snow season droughts, snowmelt droughts, and composite droughts with multiple contributing factors). The methodology relies on a hierarchical decision tree that first determines whether a drought is rainfall-driven or snow-driven and applies specific criteria to distinguish between subtypes within each category (Fig. 2).

Rainfall-driven drought events: Rainfall-driven events are classified based on precipitation deficits occurring within six pentads before and during the drought's midpoint. Three subtypes are distinguished:

1. Rain-to-snow season drought occurs when a summer rainfall deficit (June–September) is followed by potential snow accumulation during early autumn (September–October, with temperatures below 0 °C).

2. Rainfall deficit drought occurs when no subsequent snow accumulation follows a summer deficit, or when deficits fall outside the summer period but do not persist into the dry season.

3. Wet-to-dry season drought occurs when deficits arise outside the summer period and persist into the dry season (June–September), when evapotranspiration strongly affects water availability (Teuling et al., 2013; Apurv et al., 2017; Mastrotheodoros et al., 2020).

Snow-driven drought events: These events are classified when the rainfall-based criteria are not met, relying on temperature-dependent processes and snow water equivalent (SWE) availability. Four subtypes are distinguished:

4. Cold-season drought occurs during the snow season (November–March) when potential snow accumulation is possible based on sub-zero temperatures.

5. Warm snow season drought occurs when accumulation is not possible, but evidence exists of prior snow presence and subsequent melting (indicated by positive SWE).

6. Composite drought occurs when neither accumulation nor melting criteria are satisfied, representing complex multi-factor drought conditions.

7. Snowmelt drought occurs outside the snow season, when runoff deficits coincide with insufficient SWE availability.

https://doi.org/10.5194/egusphere-2026-973
Preprint. Discussion started: 4 March 2026

2.5 Model evaluation and change assessment

To evaluate both model performance and climate-driven shifts in drought-generating processes, we analyzed biases and projected changes in drought duration, severity, and frequency for each drought event type. These three metrics capture complementary aspects of hydrological stress (intensity, persistence, and recurrence) that are directly relevant for water management and impact assessment. Biases and projected changes were derived from simulations driven by five Global Climate Models (GCMs; Table 1): MIROC, GFDL, HadGEM2, IPSL, and NorESM, so that the ensemble mean provides a robust summary of model behavior. Bias was quantified as the difference in drought characteristics between EOBS and GCM-driven simulations for the historical period 1971–2000. Specifically, relative bias (%) was calculated as $(\text{observed} - \text{historical})/\text{observed} \times 100$, -where negative values indicate underestimation of corresponding drought characteristic (i.e., event duration, severity/runoff deficit, or event frequency) by the GCM-forced simulation relative to the EOBS reference. Projected changes were assessed by comparing future GCM simulations for 2070–2099 with their respective historical counterparts. Relative change (%) was defined as $(\text{future} - \text{historical})/\text{historical} \times 100$, representing the percentage difference in drought metrics under future climate scenarios. Changes in drought generation processes were assessed by applying the same seven-type runoff drought classification to each dataset (EOBS, `GCM_hist`, and `GCM_fut`) and then evaluating, for each drought type, how the mean event duration, mean number of events, and mean severity/deficit differ between the historical and future simulations. This type-wise comparison provides a direct measure of shifts in the characteristics of individual processes (rather than only aggregated drought behavior), and the EOBS–historical comparison serves as a benchmark for historical performance. Furthermore, the Getis–Ord G_i^* statistic was applied to identify statistically significant spatial clusters of drought mechanisms, enabling the detection of coherent regional patterns in drought typology distribution. This local spatial autocorrelation measure evaluates whether specific drought types are spatially concentrated (severe positive) or dispersed (severe negative) by comparing each grid cell's characteristics with those of its neighbors. The mathematical formulation of this spatial autocorrelation analysis is provided in the Appendix A.

3 Results

3.1 Assessment of biases in GCM simulations (1971–2000)

Global Climate Models demonstrate robust capability in reproducing the observed fractional contribution (percentage share) of each drought type to the total number of drought events, despite underestimating the absolute number of events. Table 3 presents the number of drought events and their typological distribution across observational data (EOBS, 1971–2000) and five GCMs (MIROC, GFDL, HadGEM2, IPSL, NorESM) under the RCP4.5 scenario. All models successfully reproduce the dominance of rainfall deficit events, which account for 60–70% of total drought occurrences, closely aligning with the observed fraction of 64.7%. While rainfall deficit droughts dominate both observations and simulations (63.4–69.9%), they exhibit relative frequency biases ranging from –36.0% to –27.4%, indicating systematic underestimation in absolute event frequencies. Rain-to-Snow droughts show the lowest biases among typologies, ranging from –48.2% to –0.2%, whereas snowmelt and

https://doi.org/10.5194/egusphere-2026-973
Preprint. Discussion started: 4 March 2026

composite droughts are significantly underrepresented in the simulations, with relative biases between –82.1% and –33.5%. Notably, composite events constitute less than 1% of total events in both observations and model outputs. Among the GCMs, IPSL exhibits the most balanced performance, with moderate and consistent biases across all drought categories, whereas MIROC shows mixed results, with some low biases but also instances of strong underestimation.

Following the individual model assessment, we constructed an ensemble mean from all five GCMs to provide a more robust estimate of historical biases and future changes in key drought characteristics, namely event frequency, duration, and runoff deficit severity. Our spatial analysis of mean runoff deficit biases reveals pronounced regional heterogeneity, with severe underestimation of runoff deficits related to rain-to-snow droughts in northern Europe. While models generally capture observed spatial patterns, systematic biases emerge across drought event types and regions (Fig. 3). EOBS observations indicate moderate deficits (-2 to $-3\,\mathrm{mm\,day^{-1}}$) in Mediterranean regions for rainfall deficit droughts, while rain-to-snow events show the most severe deficits exceeding $-4\,\mathrm{mm\,day^{-1}}$ in northern Europe. Critically, the modelled severity of rain-to-snow droughts is underestimated in northern Europe, with biases up to $4.5\,\mathrm{mm\,day^{-1}}$ (Figure 3c). Regional analysis shows pronounced negative biases for temperature-dependent drought event types in NEU and WCE (median -6 to $-8\,\mathrm{mm\,day^{-1}}$), while Mediterranean regions display more moderate values (Figure 3d). Despite these biases in absolute drought characteristics relative to EOBS, all subsequent analyses of future change are based exclusively on comparisons between historical and future GCM simulations, which share the same systematic bias structure. The consistent spatial patterns and relative distributions of drought event types across models therefore support the robustness of the assessed relative changes. Similar underestimation is evident for mean duration and mean number of events (Supplementary Figures S4–S5).

https://doi.org/10.5194/egusphere-2026-973
Preprint. Discussion started: 4 March 2026

Table 3. Comparison of drought events between GCMs (RCP4.5) and EOBS (1971–2000), categorised by drought event type. *Number of events* refers to absolute counts in EOBS (N_{OBS}) or historical GCM simulations (N_{hist}). *Fraction of events* (%) indicates the proportion of each drought event type relative to the total event count per dataset. *Relative bias* (%) is calculated as $(N_{OBS} - N_{hist})/N_{OBS} \times 100$, representing the percentage difference between modelled and observed event counts. Negative values indicate underestimation by the model.

Metrics	Rainfall Deficit	Rain to Snow	Wet to Dry	Warm Snow	Cold Snow	Snowmelt	Composite
EOBS v25 observations							
Number of events	30993	3400	5273	957	2793	3952	475
Fraction of events (%)	64.7	7.1	11.0	2.0	5.8	8.2	0.9
MIROC							
Number of events	22222	2623	5243	682	1914	2110	121
Fraction of events (%)	63.6	7.5	15.0	2.0	5.4	6.4	0.3
Relative bias (%)	-28.3	-22.8	-0.6	-28.7	-31.5	-46.6	-74.6
GFDL							
Number of events	19842	3394	4414	476	1384	1725	85
Fraction of events (%)	63.4	10.8	14.1	1.5	4.4	5.5	0.3
Relative bias (%)	-36.0	-0.2	-16.3	-50.3	-50.4	-56.4	-82.1
HadGEM2							
Number of events	20992	2740	4681	561	2060	1952	96
Fraction of events (%)	63.5	8.3	14.1	1.7	6.2	5.9	0.3
Relative bias (%)	-32.3	-19.4	-11.2	-41.4	-26.2	-50.6	-79.8
IPSL							
Number of events	22502	2395	3848	572	1532	2663	251
Fraction of events (%)	66.6	7.1	11.4	1.7	4.5	7.9	0.7
Relative bias (%)	-27.4	-29.6	-27.1	-40.3	-45.1	-32.7	-47.2
NorESM							
Number of events	22412	1762	3933	458	1490	1674	316
Fraction of events (%)	69.9	5.5	12.3	1.4	4.6	5.2	0.9
Relative bias (%)	-27.7	-48.2	-25.4	-52.1	-46.7	-57.6	-33.5

https://doi.org/10.5194/egusphere-2026-973
Preprint. Discussion started: 4 March 2026

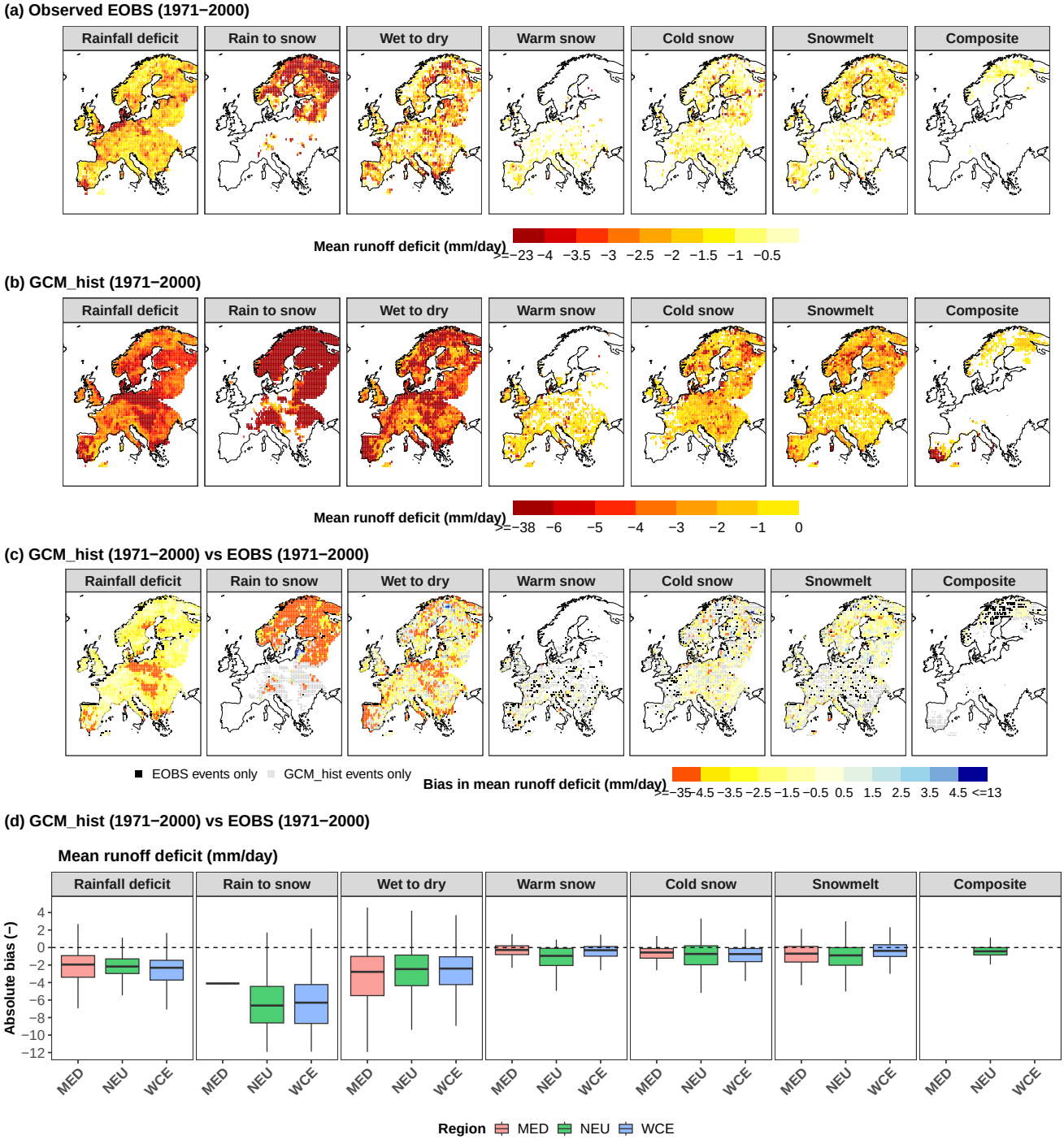

Figure 3. Assessment of bias in mean runoff deficit (mm day^{-1}) for different drought event types. (a) observed EOBS data (1971–2000); (b) ensemble mean runoff deficit for historical GCM simulations (GCM_{hist}, 1971–2000); (c) bias in mean runoff deficit between GCM_{hist} and EOBS; and (d) absolute bias for mean runoff deficit (mm day^{-1}) in historical GCM simulations relative to EOBS observations for three IPCC reference regions (MED, NEU, WCE) and each drought event type. Results are derived from an ensemble of five GCMs.

https://doi.org/10.5194/egusphere-2026-973
Preprint. Discussion started: 4 March 2026

3.2 Projected changes in drought characteristics

Projected changes in drought events under RCP4.5 reveal contrasting responses across Europe (Tab. 4) in terms of changes in drought event frequency and relative event-type composition. Relative to the historical period (GCM_hist) (1971–2000), the frequency of rainfall-deficit events increases substantially in (GCM_fut) (2070-2099), with relative changes ranging from +13% to +116% across models. Wet-to-dry, warm-snow, and snowmelt droughts also become more frequent, showing increases of +8% to +167%. In contrast, the frequency of cold-snow droughts consistently declines by -28% to -84%, reflecting the strong influence of warming on snow-dominated processes. These systematic shifts indicate that while snow-related droughts become less frequent, rainfall-driven and transitional droughts become more prevalent across much of Europe.

Runoff deficits intensify under future climate conditions, with the Mediterranean emerging as the hotspot of intensification (Figure 4). Historical simulations (Fig. 4a) show the largest deficits for rain-to-snow events in Northern Europe (exceeding -7 mm day^{-1}) and moderate deficits for rainfall-deficit events in the Mediterranean (-3 to -5 mm day^{-1}) (Spinoni et al., 2016). Future simulations (Figure 4b) of ensemble mean runoff deficit indicate stronger deficits across most drought event types, particularly rainfall-deficit and wet-to-dry events, which intensify across Central and Southern Europe, with particularly pronounced increases in the Mediterranean basin (Samaniego et al., 2018; Cook et al., 2016). Snow-related droughts exhibit mixed patterns, with some regions experiencing reduced deficits due to changing snowpack dynamics under warming conditions, while others maintain or slightly increase their deficit magnitudes until the end of this century. The spatial pattern of projected changes (Fig. 4c) highlights strong runoff deficit increases in the Mediterranean, moderate increases in Western–Central Europe due to reduced snowpack and earlier melt (Laaha et al., 2017), and relative resilience in Northern Europe.

Regional quantification (Fig. 4d) further confirms these disparities, with rainfall-deficit droughts in the Mediterranean intensifying by about -5 to -7 mm day^{-1}. A notable contrast is observed in the rain-to-snow category, where Western–Central Europe shows positive median values (around +3 mm day^{-1}), suggesting reduced deficit severity for this drought event type. Temperature-dependent drought types (warm snow, cold snow, and snowmelt-related droughts) exhibit relatively small projected changes across all regions. Median changes are close to zero, and the spread of the results is limited, indicating a stable response under the projected warming signal in the future climate simulations. These regional disparities emphasize the critical influence of snow-dominated regimes in shaping future runoff deficits. In the Mediterranean, the hydrological response to climate forcing is particularly pronounced, with rainfall deficit intensification of 5–7 mm day^{-1} indicating a fundamental shift in regional water balance dynamics.

Projected changes in drought duration reveal a pronounced north–south gradient, with the strongest increases in the Mediterranean (Fig. 5). During the historical period, droughts in the Mediterranean often exceeded 200 days, whereas much shorter durations prevailed in Northern Europe. Projections for 2070–2099 (GCM_fut) indicate substantial increases in drought duration in the Mediterranean, particularly for rainfall-deficit droughts, where durations may lengthen by more than 200 days due to enhanced evapotranspiration and reduced precipitation. In contrast, West-Central Europe shows moderate increases in duration (approx 25–75 days), with changes affecting both rainfall and temperature-influenced drought types, including snow-related

https://doi.org/10.5194/egusphere-2026-973
Preprint. Discussion started: 4 March 2026

events associated with reduced snowpack persistence and earlier melt. while Northern Europe remains comparatively stable, with changes typically within ±25 days. Figure 5d further illustrates that the Mediterranean faces both the most extreme mean increases in duration and the widest uncertainty range, Northern Europe the tightest and smallest variability, and West-Central Europe showing intermediate values.

Table 4. Comparison of drought events between future GCM simulations (2070–2099, RCP4.5) and historical GCM simulations (1971–2000), categorised by drought event type. *Number of events* refers to absolute counts in future GCM simulations (N_{fut}). *Relative change* (%) is calculated as $(N_{fut} - N_{hist})/N_{hist} \times 100$, representing the percentage difference between future and historical event counts. Positive values indicate an increase and negative values indicate a decrease in event frequency under future climate conditions.

Metrics	Rainfall Deficit	Rain to Snow	Wet to Dry	Warm Snow	Cold Snow	Snowmelt	Composite
MIROC							
Number of events	29083	1122	7454	1033	312	3454	–
Relative change (%)	+31	-57	+42	+51	-84	+64	–
GFDL							
Number of events	22501	897	5211	651	825	1975	5
Relative change (%)	+13	-74	+18	+37	-40	+14	-94
HadGEM2							
Number of events	45400	2898	6328	1251	1475	3663	197
Relative change (%)	+116	+6	+35	+123	-28	+88	+105
IPSL							
Number of events	43787	1627	6887	940	385	3621	375
Relative change (%)	+95	-32	+79	+64	-75	+36	+49
NorESM							
Number of events	48232	4205	4259	1222	1050	3792	252
Relative change (%)	+115	+139	+8	+167	-30	+127	-20

Changes in the number of drought events further amplify the spatial disparities, with the Mediterranean experiencing the largest increases across drought types (Fig. 6). Rainfall-deficit events rise by about +3 to +4 in this region, while wet-to-dry transitions also become more frequent, reflecting increasingly erratic precipitation seasonality and stronger evaporative demand (Teuling et al., 2013; Spinoni et al., 2018). Western-Central Europe shows moderate increases (+1 to +2 events) in snowmelt and warm-snow droughts, linked to reduced snowpack and earlier melt timing (Van Loon and Van Lanen, 2012). Northern Europe displays stable to slightly declining counts (-1 to 0 events) for cold-snow droughts, though minor shifts are evident in composite drought events. Overall, these changes confirm the Mediterranean as Europe's primary drought change hotspot, highlight emerging vulnerabilities in snow-dependent regions of Western-Central Europe (WCE), and suggest continued resilience in Northern Europe (NEU).

https://doi.org/10.5194/egusphere-2026-973
Preprint. Discussion started: 4 March 2026

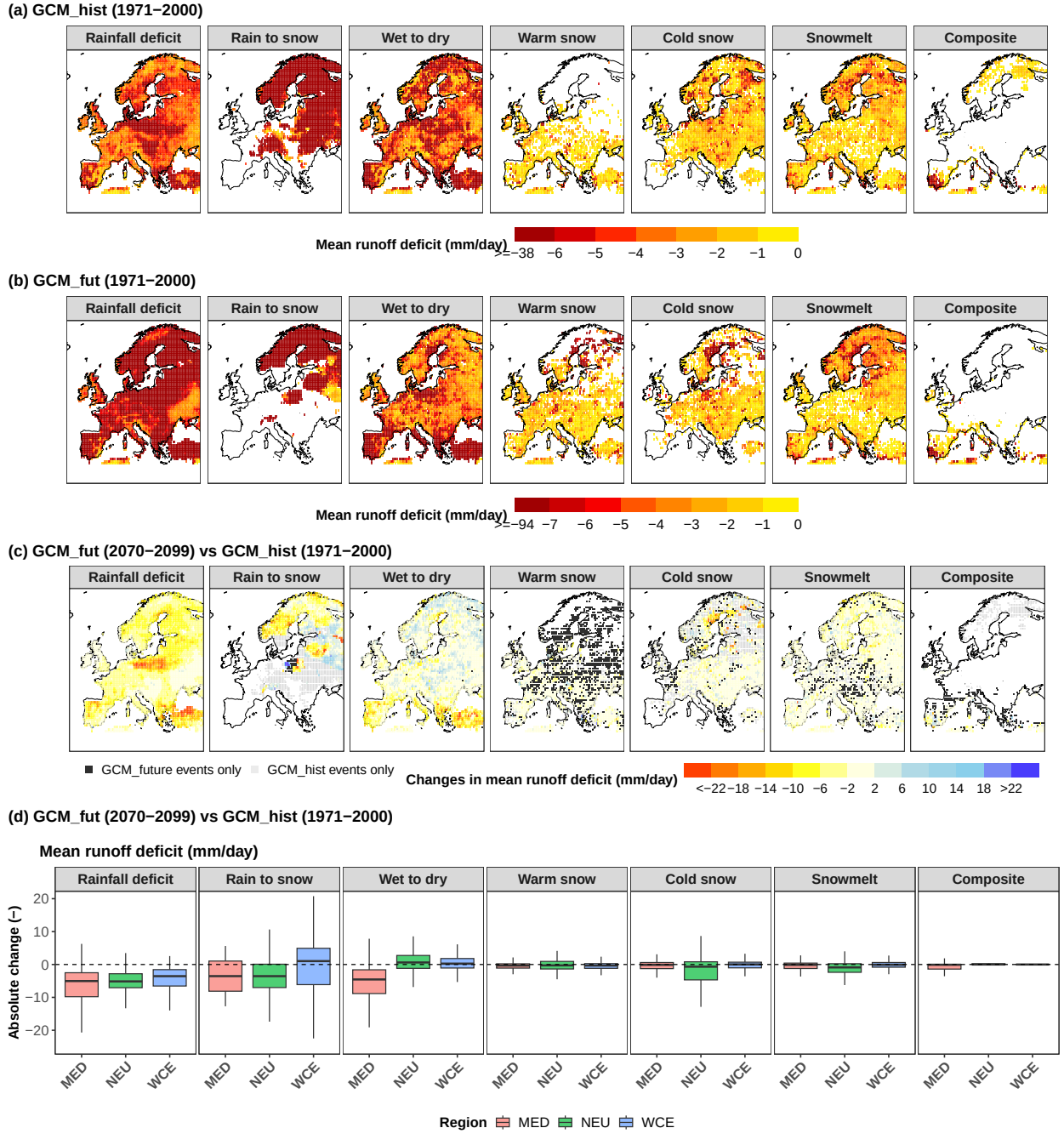

Figure 4. Assessment of changes in mean runoff deficit (mm day^{-1}) for different drought event types. (a) ensemble mean runoff deficit for historical GCM simulations (GCM_{hist}, 1971–2000); (b) ensemble mean runoff deficit for future GCM simulations (GCM_{hist}, 2071–2099); (c) changes in mean runoff deficit between GCM_{hist} and GCM_{fut}; and (d) absolute changes for mean runoff deficit (mm day^{-1}) between historical and projected GCM simulations for three IPCC reference regions (MED, NEU, WCE) and each drought event type.

https://doi.org/10.5194/egusphere-2026-973
Preprint. Discussion started: 4 March 2026

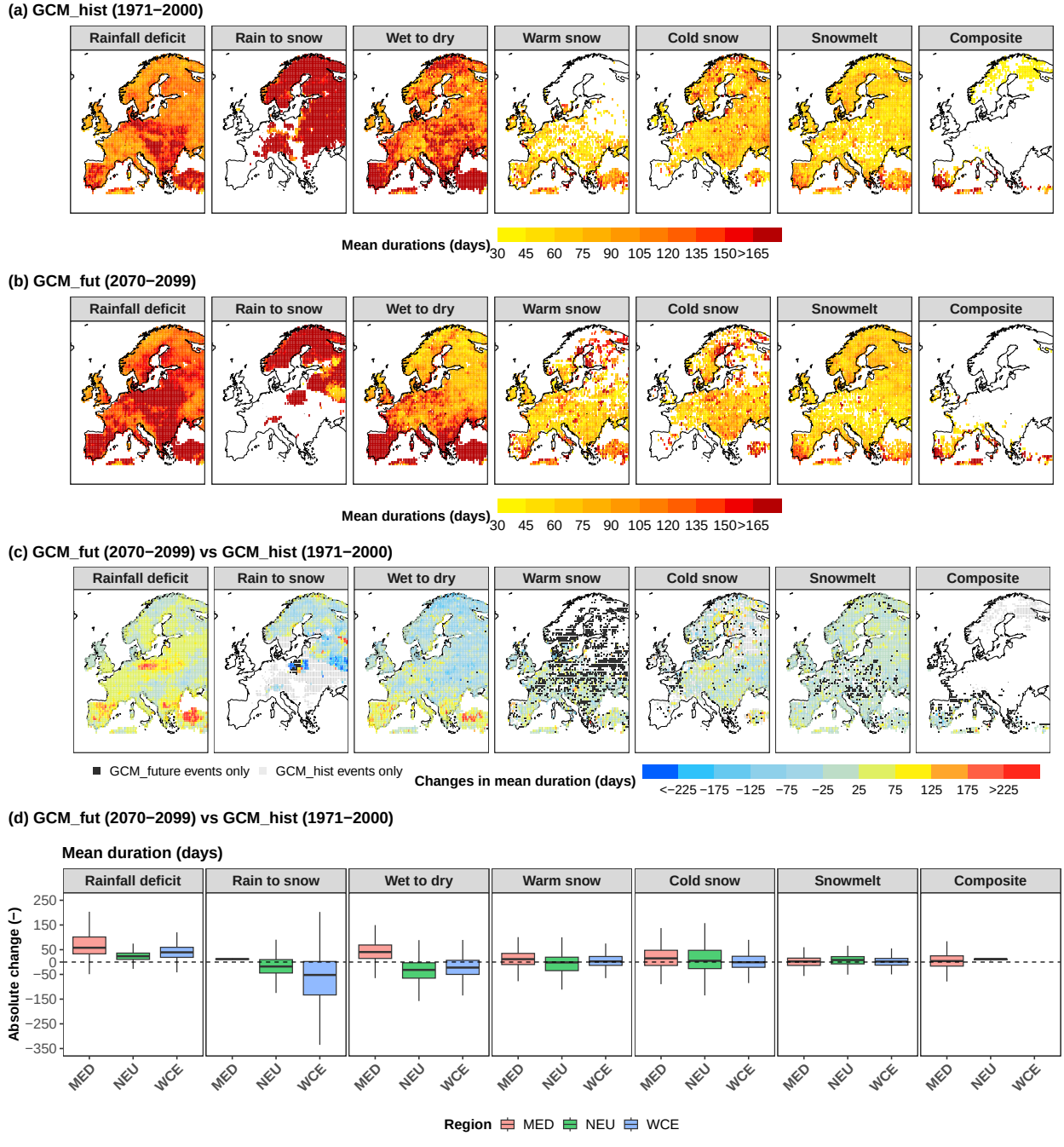

Figure 5. Assessment of changes in mean duration (days) for different drought event types. (a) ensemble mean duration for historical GCM simulations (GCM_{hist}, 1971–2000); (b) ensemble mean duration for future GCM simulations (GCM_{hist}, 2071–2099); (c) changes in mean duration between GCM_{hist} and GCM_{fut}; and (d) absolute changes for mean duration (days) between historical and projected GCM simulations for three IPCC reference regions (MED, NEU, WCE) and each drought event type.

https://doi.org/10.5194/egusphere-2026-973
Preprint. Discussion started: 4 March 2026

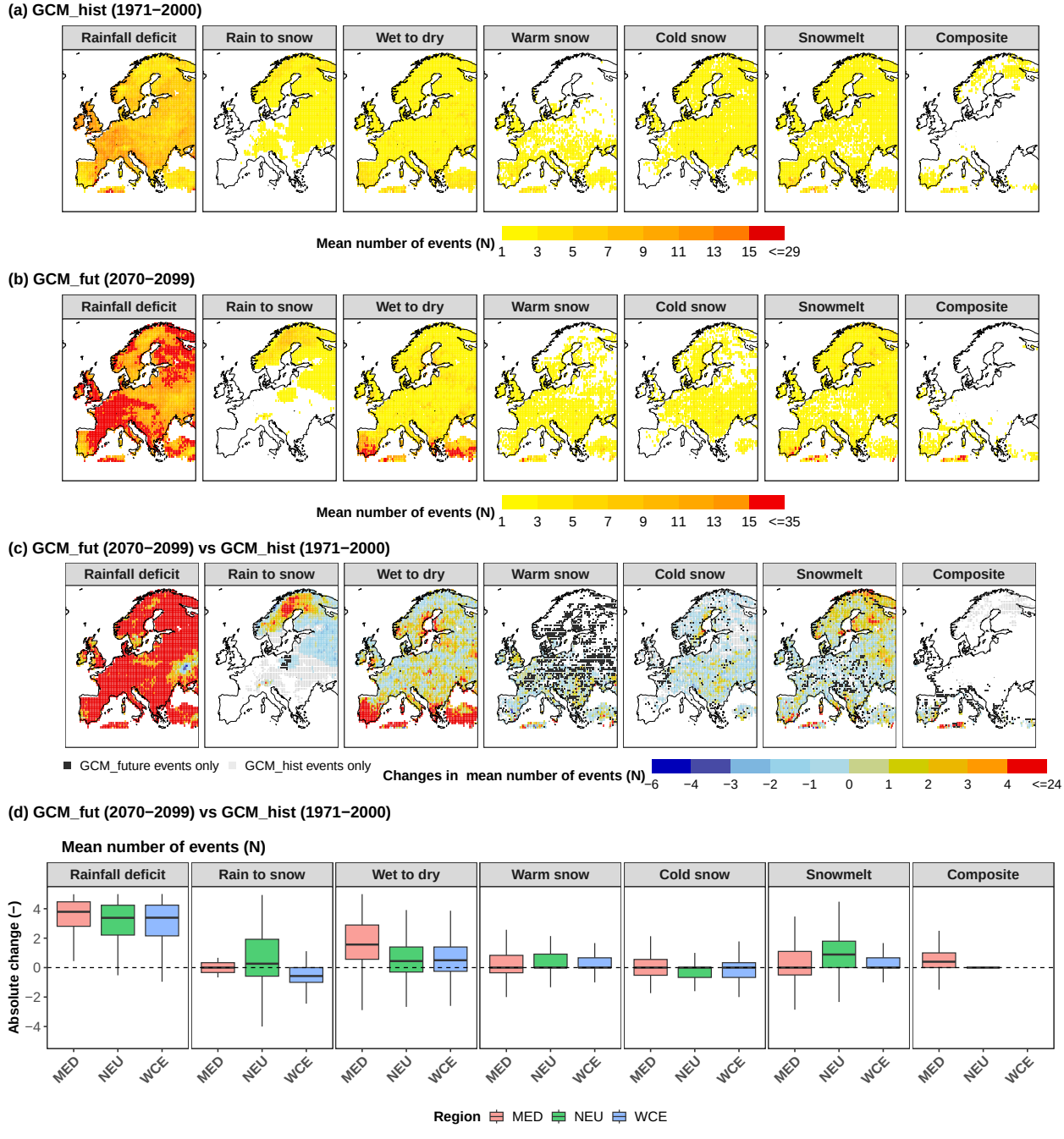

Figure 6. Assessment of changes in mean number of events (–) for different drought event types. (a) ensemble mean number of events for historical GCM simulations (GCM_{hist}, 1971–2000); (b) ensemble mean mean number of events for future GCM simulations (GCM_{hist}, 2071–2099); (c) changes in mean number of events between GCM_{hist} and GCM_{fut}; and (d) absolute changes for mean number of events between historical and projected GCM simulations for three IPCC reference regions (MED, NEU, WCE) and each drought event type.

https://doi.org/10.5194/egusphere-2026-973
Preprint. Discussion started: 4 March 2026

3.3 Hotspot analysis of drought classifications

Our spatial hotspot analysis identifies the Mediterranean basin as a statistically robust center of compound drought intensification, whereas northern European regions show more heterogeneous, drought-type-specific responses to climate forcing (Fig. 7). Future change analysis (`GCM_fut`, 2070–2099 vs. `GCM_hist`, 1971–2000) shows strong spatial clustering of projected drought intensification primarily over the western Mediterranean, with positive side hotspots most consistently detected over the Iberian Peninsula for all three drought characteristics: mean runoff deficit, drought duration, and number of events (Fig. 7). In contrast, other Mediterranean regions, including southern France and Italy, display weaker and more localized hotspot patterns that are largely drought-type specific, most notably for rainfall-deficit and wet-to-dry transition droughts. These areas, which are already vulnerable to seasonal water stress (Vautard et al., 2014; Kumar et al., 2025; Seneviratne et al., 2021), are projected to face compound drought hazards, characterized by simultaneous intensification in deficit, duration, and event frequency, representing a convergence of multiple drought-generating mechanisms that further amplifies regional vulnerability. In contrast to the Mediterranean's consistent intensification, Central Europe exhibits transitional, fragmented hotspot patterns in drought characteristics, with weak model agreement, reflecting complex interactions between shifting precipitation and declining snowpack. In contrast, northern Europe displays spatially heterogeneous and drought-type-dependent patterns, with both positive and negative anomalies emerging, reflecting complex hydrological responses to altered precipitation regimes, snow dynamics, and seasonal runoff under a warming climate (Jacob et al., 2014; Staudinger et al., 2014; Van Loon and Van Lanen, 2012; Van Loon, 2015).

https://doi.org/10.5194/egusphere-2026-973
Preprint. Discussion started: 4 March 2026

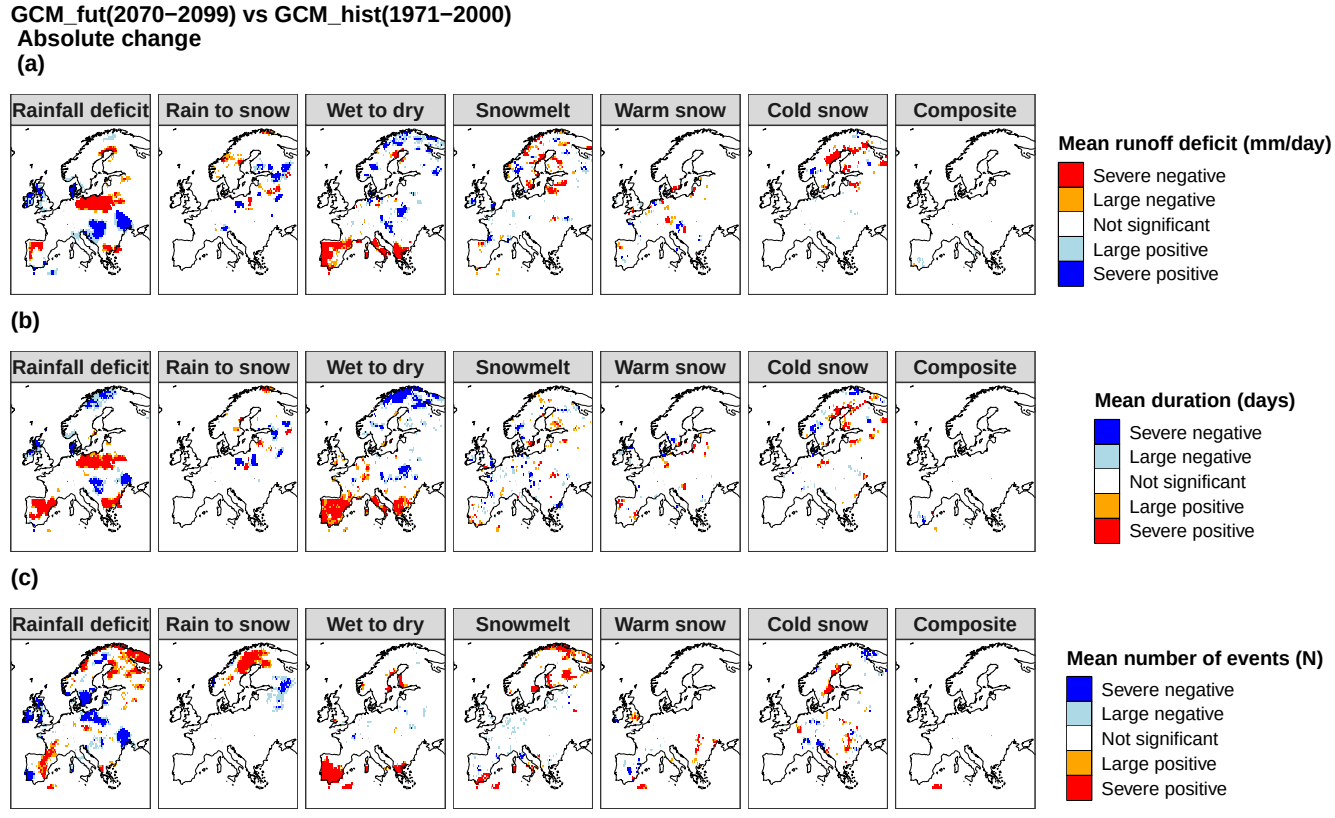

Figure 7. Getis-Ord G_i^* hotspot analysis of projected absolute changes in GCM simulations (`GCM_fut`, 2070–2099 relative to `GCM_hist`, 1971–2000) across European grid cells, disaggregated by drought event type. Panels show spatial clusters of change in (a) mean runoff deficit (mm day^{-1}), (b) mean drought duration (days), and (c) mean number of drought events. Colors indicate statistically significant positive and negative hotspots, with darker shades reflecting more severe changes.

3.4 Drought event timing

Our results show that seasonal drought timing across Europe follows distinct regional patterns that remain consistent under climate change (Fig. 8). EOBS (1970–2000) observations reveal distinct regional patterns in drought timing across Europe. The Mediterranean shows rainfall deficit droughts starting in May–June with drought termination in June, indicating short-duration events of 1–2 months. Western Central Europe shows similar initiation times in May–June but slightly later termination in June–July. Northern Europe exhibits the latest drought onsets (June–July) and termination in June–July, representing the most constrained seasonal window. Wet-to-dry transition events generally start in early spring (March–April) and persist into late summer (August–September), establishing approximately 5-month duration cycles. Snow-related droughts occur prominently in Western Central Europe and Northern Europe during March–April, with less frequent occurrence in the Mediterranean. Overall, rainfall deficit events are short (1–2 months), while wet-to-dry transitions are longer (≈ 5 months).

https://doi.org/10.5194/egusphere-2026-973
Preprint. Discussion started: 4 March 2026

Historical GCM simulations `GCM_hist` (1970–2000) broadly reproduce the seasonal drought signatures identified in EOBS observations, though with some systematic deviations (Fig. 8). The model shows a slight delay in Mediterranean rainfall deficit initiation (June–July vs EOBS May–June), while maintaining consistent termination timing. Snow-related droughts show a higher seasonal occurrence in the Mediterranean compared to observation, indicating increased persistence within the seasonal cycle rather than an overestimation of absolute event frequency, which is underestimated overall Table 3. In contrast, Western Central Europe and Northern Europe regions show good agreement with EOBS patterns for most drought event types. Overall, `GCM_hist` exhibits minimal temporal biases with primary discrepancies occurring in Mediterranean drought timing and the frequency of snow droughts.

Future projections `GCM_fut` (2070–2099) indicate an intensification and prolongation of drought regimes rather than fundamental shifts in seasonal timing (Fig. 8). Rainfall deficit droughts maintain their regional timing pattern (MED: June–July, WCE: May–June, NEU: June–July) but evolve from short 1–2 month events into longer drought seasons of 3–4 months. Wet-to-dry transition droughts continue to span the full warm season but increase in frequency and severity. Snow-related droughts show the most consistent temporal shift, with onset advancing from March–April to February–March, reflecting the influence of warming on snow accumulation and melt processes. Overall, the temporal analysis suggests that the seasonal timing of European droughts remains stable under climate change, but with longer durations and higher intensities.

https://doi.org/10.5194/egusphere-2026-973
Preprint. Discussion started: 4 March 2026

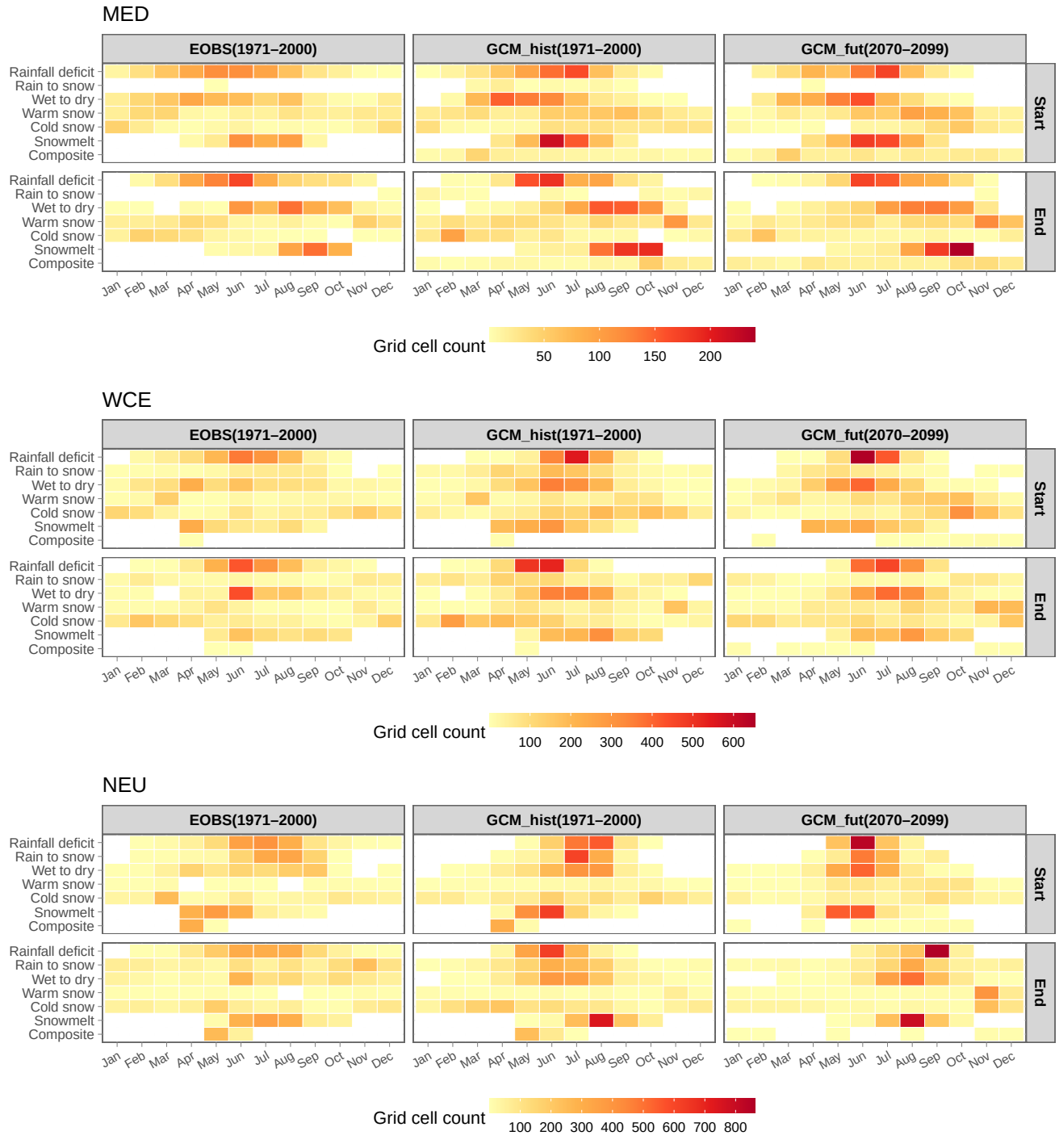

Figure 8. Heatmap representation of (a) drought start and (b) ends across reference (1971–2000) and future (2070–2099) periods under RCP4.5. Each tile shows the grid cell count corresponding to the average start or end month for a given drought event type.

https://doi.org/10.5194/egusphere-2026-973
Preprint. Discussion started: 4 March 2026

4 Discussion

Understanding how distinct drought-generating processes respond to climate forcing across Europe is critical for anticipating regional water risks and guiding adaptation strategies. The historical evaluation reveals systematic biases in GCM-driven simulations of runoff-deficit droughts, characterized by underestimated event frequency and overestimated event severity. These co-occurring biases are physically consistent and reflect a common behavior of hydrological droughts, whereby longer and more persistent runoff deficits allow deficit volumes to accumulate, leading to higher severity per event (Van Loon, 2015). Importantly, future changes are assessed exclusively through comparisons between historical and future GCM simulations, which share the same structural bias characteristics, ensuring internally consistent relative changes (Gudmundsson and Seneviratne, 2016).

Our classification of seven drought event types under moderate warming (RCP4.5) shows that temperature-sensitive categories, particularly rain-to-snow and warm-snow droughts, exhibit the strongest projected increases in both runoff deficit ($mm\,day^{-1}$) and number of events (N) (Fig. 4, Fig. 6; Table 4). In contrast, cold-snow droughts decline by -28% to -84% in frequency, confirming that thermodynamically unstable processes are most responsive to warming. These results align with previous findings that droughts governed by phase-transition processes are highly sensitive to even modest temperature increases (Musselman et al., 2021; Van Loon and Van Lanen, 2012; Van Loon, 2015).

Building on this continental-scale classification, spatial patterns reveal clear regional reorganizations in drought-generating processes. The Mediterranean basin emerges as the primary hotspot of multi-process drought intensification, with mean runoff deficit increases exceeding $+7\,mm\,day^{-1}$ and event durations extending beyond 200 days (Fig. 4, Fig. 5). This pattern points to a convergence of drought-generating mechanisms, with several event types strengthening at the same time and intensifying regional hydrological stress. This co-occurrence is consistent with the hypothesis that climate impacts are often amplified by *compound events*, i.e., the concurrence of multiple drivers (e.g., precipitation deficits with enhanced evaporative demand and related hydrological feedbacks) leading to disproportionate increases in severity and duration (Zampieri et al., 2017; Seneviratne et al., 2012). This interpretation is supported by event-based evidence that extreme evaporation episodes arise from distinct energy–moisture configurations and can amplify hydrological deficit accumulation when coincident with precipitation shortfalls, reinforcing compound drought intensification (Markonis, 2025).

In contrast, Western–Central Europe shows a transition from cold-snow toward rain-to-snow dominated droughts, reflecting reduced snowpack and earlier melt, while Northern Europe, although largely stable in total drought metrics (duration, severity and number of events), reveals internal shifts in event-type composition. Together, these contrasting trajectories underscore a continent-wide shift in drought-process regimes across Europe, with Mediterranean regions facing compounding drought pressures, Central Europe transitioning toward thermally-driven regimes characterized by reduced snowpack, earlier snowmelt, and enhanced evaporative demand, and Northern Europe showing comparatively modest shifts in drought processes.

The analysis of spatial pattern changes aligns with previous projections by Seneviratne et al. (2021), which identify the Mediterranean as Europe's primary drought vulnerability hotspot, driven by concurrent declines in rainfall and rising temperatures. Consistent with CMIP6 projections of longer and more frequent droughts in this region (Spinoni et al., 2020; Shah

https://doi.org/10.5194/egusphere-2026-973
Preprint. Discussion started: 4 March 2026

et al., 2022), our spatial hotspot analysis (Fig. 7) statistically highlights Southern Europe as the main center of multi-typology drought intensification, providing a spatial basis for targeted adaptation planning. Temporal characteristics reinforce this signal: drought seasons in the Mediterranean start earlier and last longer, particularly for rainfall-deficit events (Fig. 8), in line with projections of pronounced summer drying linked to stronger anticyclonic circulation, a northward shift of the Atlantic storm track, and amplified summer warming (Giorgi and Lionello, 2008). CMIP5/CMIP6 show amplified summer warming and robust precipitation declines over the Mediterranean, and these signals remain when models are weighted for performance and inter-dependence, strengthening confidence in elevated drought risk for Southern Europe (Cos et al., 2022).

From a modeling perspective, our multi-model ensemble across five GCMs reveals consistent underestimation of runoff deficit of temperature-sensitive drought event types in the historical baseline (Fig. 3), particularly for rain-to-snow and warm-snow categories. This structural bias suggests that current GCMs may insufficiently capture phase-transition thresholds in hydrological processes due to topographical shifts and the snow melting processes, a well-documented challenge in climate model physics (Xu et al., 2024; Imura and Michibata, 2022). These findings highlight the need for drought monitoring systems to account for shifting event types, particularly those involving temperature-controlled shifts between snow and rain and the timing of snowmelt. Rain-to-snow shifts, for instance, require real-time detection of temperature thresholds in addition to cumulative precipitation totals, therefore benefiting from higher-resolution climate inputs, such as those available from regional climate model ensembles within EURO-CORDEX (Jacob et al., 2014)). Overall, the multi-model ensemble consistently indicates a shift toward longer and severe droughts, with strong regional contrasts (Figs. 4 and 5).

Finally, some limitations should be acknowledged to frame the scope of these findings. The pentad-scale temporal resolution may under-represent rapidly developing droughts that are primarily expressed through soil moisture and evapotranspiration dynamics, whose runoff responses are often delayed or attenuated (Shah et al., 2022). On top of this, estimates of enhanced evaporative demand and their inferred trends can be sensitive to the choice of PET formulation, implying that drought attribution involving “increased demand” should be treated with caution due to PET-method sensitivity (Thakur et al., 2025). Our framework does not capture compound drought events or cascade interactions-an important future research direction given their increasing prevalence under climate extremes (Gesualdo et al., 2024). While the focus on RCP4.5 provides a plausible mid-range pathway, more severe emissions scenarios could trigger nonlinear regime shifts not reflected here (Lehner et al., 2017). In addition, the exclusion of anthropogenic influences such as land use change and water withdrawals may limit process realism at regional scales. We present CMIP5/ISIMIP2b results as a showcase; the framework itself is generic and transferable to CMIP6/ISIMIP3b forcings and it provides a basis for extension to other scenario ensembles in future work (i.e EURO-CORDEX (Jacob et al., 2014)). Applying it to higher-resolution CMIP6 ensembles will allow for a sharper test of model spread and regional signals while keeping the same event-type definitions and diagnostics. Nevertheless, our process-based classification provides new insights into how distinct drought processes may evolve under climate change across Europe, and these insights can inform next-generation drought risk assessments, monitoring strategies, and adaptation policies.

https://doi.org/10.5194/egusphere-2026-973
Preprint. Discussion started: 4 March 2026

5 Conclusions

We applied a process-based framework to study drought generation mechanisms, combining local drought event classification with spatial clustering analysis to assess drought responses to climate forcing across Europe. This methodology has broader applicability beyond our study area, as it can be transferred to investigate process-based drought changes in other regions. The drought classification were prepared using the R-code below and can be accessed at free, public repository Zenodo (https://doi.org/10.5281/zenodo.18479544). For Europe, we identified seven distinct drought event types with contrasting climate sensitivities and regional distributions. The Mediterranean region experiences the strongest drought intensification, with runoff deficit increases of 2–6 mm day^{-1} and duration extensions exceeding 200 days, while Northern Europe shows predominantly stable characteristics. Temperature-driven processes, particularly rain-to-snow transitions, exhibit the most pronounced projected changes across all drought metrics. Spatial clustering further reveals significant aggregation of drought intensification in the Mediterranean basin, underscoring its susceptibility to compound multi-process drought risks under moderate warming scenarios.

Appendix A: Statistical assessment of spatial association: the Getis–Ord G_i^* method

The Getis–Ord G_i^* statistic (Getis and Ord, 1992) evaluates spatial clustering by comparing local spatial relationships with global patterns. For a given location i, the G_i^* statistic is defined as:

$$G_i^* = \frac{\sum_{j=1}^{n} w_{ij}x_j - \bar{X}\sum_{j=1}^{n} w_{ij}}{S\sqrt{\frac{n\sum_{j=1}^{n} w_{ij}^2 - (\sum_{j=1}^{n} w_{ij})^2}{n-1}}} \tag{A1}$$

where x_j is the attribute value for feature j, w_{ij} is the spatial weight between features i and j, n is the total number of features, $\bar{X}$ is the global mean, and S is the standard deviation, calculated as:

$$S = \sqrt{\frac{\sum_{j=1}^{n} x_j^2}{n} - (\bar{X})^2}.$$

The spatial weights matrix is defined as:

$$w_{ij} = \begin{cases} 1 & \text{if feature } j \text{ is within distance } d \text{ of feature } i \\ 0 & \text{otherwise} \end{cases} \tag{A2}$$

https://doi.org/10.5194/egusphere-2026-973
Preprint. Discussion started: 4 March 2026

The local mean for location i is given by $\frac{\sum_{j=1}^{n} w_{ij}x_j}{\sum_{j=1}^{n} w_{ij}}$, which is compared with the global mean $\bar{X}$. The variance under the null hypothesis of no spatial clustering is:

$$\mathrm{Var}(G_i^*) = \frac{n\sum_{j=1}^{n} w_{ij}^2 - (\sum_{j=1}^{n} w_{ij})^2}{n-1} \tag{A3}$$

The G_i^* statistic follows a standard normal distribution, with the probability of observing a particular z-score given by:

$$P(Z \leq z) = \int_{k=-\infty}^{z} \frac{1}{\sqrt{2\pi}} e^{-k^2/2} dk \tag{A4}$$

This framework enables the identification of statistically significant spatial clusters, where positive z-scores indicate hot spots and negative z-scores indicate cold spots, with the magnitude reflecting the intensity of clustering.

Author contributions. The study was initially designed by SN and MH.Hydrological simulations were performed by OR. All post-processing algorithms were coded by SN with the assistance of MH, OR, US. SN wrote the first draft of the study, with inputs from OR, and MH. YM, RK, and MIB helped frame the storyline, reshape the analyses and revised and edited the manuscript.

Competing interests. At least one of the (co)-authors is a member of the editorial board of Hydrology and Earth System Sciences.

Acknowledgements. This work was carried out within the DynamicDrought project no. 23-520 08056S of the Grant Agency of the Czech Republic and the bilateral project Smart Landscape 2030+ , registration number CZ.10.01.01/00/22_001/0000287. Computational resources were partly provided by the e-INFRA CZ project (ID:90254), supported by the Ministry of Education, Youth and Sports of the Czech Republic. SN was also supported by the internal grant of the Czech University of Life Sciences, Faculty of Environmental Sciences, (Project No.2021B0023). OR acknowledges the Research Excellence in Environmental Sciences (REES) project of the Faculty of Environmental Sciences, Czech University of Life Sciences Prague.

https://doi.org/10.5194/egusphere-2026-973
Preprint. Discussion started: 4 March 2026

References

Apurv, T., Sivapalan, M., and Cai, X.: Understanding the role of climate characteristics in drought propagation, Water Resources Research, 53, 9304–9329, 2017.

Barker, L. J., Hannaford, J., Chiverton, A., and Svensson, C.: From meteorological to hydrological drought using standardised indicators, Hydrology and Earth System Sciences, 20, 2483–2505, 2016.

Bevacqua, E., Rakovec, O., Schumacher, D. L., Kumar, R., Thober, S., Samaniego, L., Seneviratne, S. I., and Zscheischler, J.: Direct and lagged climate change effects intensified the 2022 European drought, Nature Geoscience, 17, 1100–1107, 2024.

Boeing, F., Rakovec, O., Kumar, R., Samaniego, L., Schrön, M., Hildebrandt, A., Rebmann, C., Thober, S., Müller, S., Zacharias, S., Bogena, H., Schneider, K., Kiese, R., Attinger, S., and Marx, A.: High-resolution drought simulations and comparison to soil moisture observations in Germany, Hydrology and Earth System Sciences, 26, 5137–5161, https://doi.org/10.5194/hess-26-5137-2022, 2022.

Brunner, M. I., Slater, L., Tallaksen, L. M., and Clark, M.: Challenges in modeling and predicting floods and droughts: A review, Wiley Interdisciplinary Reviews: Water, 8, e1520, 2021.

Brunner, M. I., Van Loon, A. F., and Stahl, K.: Moderate and severe hydrological droughts in Europe differ in their hydrometeorological drivers, Water Resources Research, 58, e2022WR032 871, 2022.

Buras, A., Rammig, A., and Zang, C. S.: Quantifying impacts of the 2018 drought on European ecosystems in comparison to 2003, Biogeosciences, 17, 1655–1672, 2020.

Ciais, P., Reichstein, M., Viovy, N., Granier, A., Ogée, J., Allard, V., Aubinet, M., Buchmann, N., Bernhofer, C., Carrara, A., et al.: Europe-wide reduction in primary productivity caused by the heat and drought in 2003, Nature, 437, 529–533, 2005.

Collins, M., Knutti, R., Arblaster, J., Dufresne, J.-L., Fichefet, T., Friedlingstein, P., Gao, X., Gutowski, W. J., Johns, T., Krinner, G., et al.: Long-term climate change: projections, commitments and irreversibility, in: Climate change 2013-The physical science basis: Contribution of working group I to the fifth assessment report of the intergovernmental panel on climate change, pp. 1029–1136, Cambridge University Press, 2013.

Cook, B. I., Anchukaitis, K. J., Touchan, R., Meko, D. M., and Cook, E. R.: Spatiotemporal drought variability in the Mediterranean over the last 900 years, Journal of Geophysical Research: Atmospheres, 121, 2060–2074, 2016.

Cornes, R. C., Van Der Schrier, G., Van Den Besselaar, E. J., and Jones, P. D.: An ensemble version of the E-OBS temperature and precipitation data sets, Journal of Geophysical Research: Atmospheres, 123, 9391–9409, 2018.

Cos, J., Doblas-Reyes, F., Jury, M., Marcos, R., Bretonnière, P.-A., and Samsó, M.: The Mediterranean climate change hotspot in the CMIP5 and CMIP6 projections, Earth System Dynamics, 13, 321–340, 2022.

Fatima, E., Kumar, R., Attinger, S., Kaluza, M., Rakovec, O., Rebmann, C., Rosolem, R., Oswald, S. E., Samaniego, L., Zacharias, S., et al.: Improved representation of soil moisture processes through incorporation of cosmic-ray neutron count measurements in a large-scale hydrologic model, Hydrology and Earth System Sciences, 28, 5419–5441, 2024.

Frieler, K., Lange, S., Piontek, F., Reyer, C. P., Schewe, J., Warszawski, L., Zhao, F., Chini, L., Denvil, S., Emanuel, K., et al.: Assessing the impacts of 1.5○ C global warming–simulation protocol of the Inter-Sectoral impact model intercomparison project (ISIMIP2b), Geoscientific Model Development, 10, 4321–4345, 2017.

Gesualdo, G. C., Benso, M. R., Mendiondo, E. M., and Brunner, M. I.: Spatially compounding drought events in Brazil, Water Resources Research, 60, e2023WR036 629, 2024.

Getis, A. and Ord, J. K.: The analysis of spatial association by use of distance statistics, Geographical analysis, 24, 189–206, 1992.

https://doi.org/10.5194/egusphere-2026-973
Preprint. Discussion started: 4 March 2026

Giorgi, F. and Lionello, P.: Climate change projections for the Mediterranean region, Global and planetary change, 63, 90–104, 2008.

Gudmundsson, L. and Seneviratne, S. I.: Anthropogenic climate change affects meteorological drought risk in Europe, Environmental Research Letters, 11, 044 005, 2016.

Hanel, M., Rakovec, O., Markonis, Y., Máca, P., Samaniego, L., Kyselỳ, J., and Kumar, R.: Revisiting the recent European droughts from a long-term perspective, Scientific reports, 8, 9499, 2018.

Hargreaves, G. H. and Samani, Z. A.: Reference crop evapotranspiration from temperature, Applied engineering in agriculture, 1, 96–99, 1985.

Hari, V., Rakovec, O., Markonis, Y., Hanel, M., and Kumar, R.: Increased future occurrences of the exceptional 2018–2019 Central European drought under global warming, Scientific reports, 10, 12 207, 2020.

Haslinger, K., Koffler, D., Schöner, W., and Laaha, G.: Exploring the link between meteorological drought and streamflow: Effects of climate-catchment interaction, Water Resources Research, 50, 2468–2487, 2014.

Hempel, S., Frieler, K., Warszawski, L., Schewe, J., and Piontek, F.: A trend-preserving bias correction–the ISI-MIP approach, Earth System Dynamics, 4, 219–236, 2013.

Huang, T.-Y., Ding, L., Yu, Y.-Q., Huang, L., and Yang, L.: From AR5 to AR6: Exploring research advancement in climate change based on scientific evidence from IPCC WGI reports, Scientometrics, 128, 5227–5245, 2023.

Imura, Y. and Michibata, T.: Too frequent and too light Arctic snowfall with incorrect precipitation phase partitioning in the MIROC6 GCM, Journal of Advances in Modeling Earth Systems, 14, e2022MS003 046, 2022.

Jacob, D., Petersen, J., Eggert, B., Alias, A., Christensen, O. B., Bouwer, L. M., Braun, A., Colette, A., Déqué, M., Georgievski, G., et al.: EURO-CORDEX: new high-resolution climate change projections for European impact research, Regional environmental change, 14, 563–578, 2014.

Kumar, R., Samaniego, L., and Attinger, S.: Implications of distributed hydrologic model parameterization on water fluxes at multiple scales and locations, Water Resources Research, 49, 360–379, 2013.

Kumar, R., Samaniego, L., Thober, S., Rakovec, O., Marx, A., Wanders, N., Pan, M., Hesse, F., and Attinger, S.: Multi-model assessment of groundwater recharge across Europe under warming climate, Earth's Future, 13, e2024EF005 020, 2025.

Kumar, R. d., Heße, F., Rao, P. S. C., Musolff, A., Jawitz, J. W., Sarrazin, F., Samaniego, L., Fleckenstein, J. H., Rakovec, O., Thober, S., et al.: Strong hydroclimatic controls on vulnerability to subsurface nitrate contamination across Europe, Nature communications, 11, 6302, 2020.

Laaha, G., Gauster, T., Tallaksen, L. M., Vidal, J.-P., Stahl, K., Prudhomme, C., Heudorfer, B., Vlnas, R., Ionita, M., Van Lanen, H. A., et al.: The European 2015 drought from a hydrological perspective, Hydrology and Earth System Sciences, 21, 3001, 2017.

Lange, S.: Trend-preserving bias adjustment and statistical downscaling with ISIMIP3BASD (v1. 0), Geoscientific Model Development, 12, 3055–3070, 2019.

Lehner, F., Coats, S., Stocker, T. F., Pendergrass, A. G., Sanderson, B. M., Raible, C. C., and Smerdon, J. E.: Projected drought risk in 1.5 C and 2 C warmer climates, Geophysical Research Letters, 44, 7419–7428, 2017.

Markonis, Y.: On the Definition of Extreme Evaporation Events, Geophysical Research Letters, 52, e2024GL113 038, 2025.

Markonis, Y., Kumar, R., Hanel, M., Rakovec, O., Máca, P., and AghaKouchak, A.: The rise of compound warm-season droughts in Europe, Science advances, 7, eabb9668, 2021.

Marx, A., Kumar, R., Thober, S., Rakovec, O., Wanders, N., Zink, M., Wood, E. F., Pan, M., Sheffield, J., and Samaniego, L.: Climate change alters low flows in Europe under global warming of 1.5, 2, and 3 C, Hydrology and Earth System Sciences, 22, 1017–1032, 2018.

https://doi.org/10.5194/egusphere-2026-973
Preprint. Discussion started: 4 March 2026

Masson-Delmotte, V., Zhai, P., Pirani, A., Connors, S. L., Péan, C., Berger, S., Caud, N., Chen, Y., Goldfarb, L., Gomis, M., et al.: Climate change 2021: the physical science basis, Contribution of working group I to the sixth assessment report of the intergovernmental panel on climate change, 2, 2391, 2021.

Mastrotheodoros, T., Pappas, C., Molnar, P., Burlando, P., Manoli, G., Parajka, J., Rigon, R., Szeles, B., Bottazzi, M., Hadjidoukas, P., et al.: More green and less blue water in the Alps during warmer summers, Nature Climate Change, 10, 155–161, 2020.

Musselman, K. N., Addor, N., Vano, J. A., and Molotch, N. P.: Winter melt trends portend widespread declines in snow water resources, Nature Climate Change, 11, 418–424, 2021.

Rakovec, O., Kumar, R., Attinger, S., and Samaniego, L.: Improving the realism of hydrologic model functioning through multivariate parameter estimation, Water Resources Research, 52, 7779–7792, 2016.

Samaniego, L., Kumar, R., and Attinger, S.: Multiscale parameter regionalization of a grid-based hydrologic model at the mesoscale, Water Resources Research, 46, 2010.

Samaniego, L., Thober, S., Kumar, R., Wanders, N., Rakovec, O., Pan, M., Zink, M., Sheffield, J., Wood, E. F., and Marx, A.: Anthropogenic warming exacerbates European soil moisture droughts, Nature Climate Change, 8, 421–426, 2018.

Samaniego, L., Thober, S., Wanders, N., Pan, M., Rakovec, O., Sheffield, J., Wood, E. F., Prudhomme, C., Rees, G., Houghton-Carr, H., et al.: Hydrological forecasts and projections for improved decision-making in the water sector in Europe, Bulletin of the American Meteorological Society, 100, 2451–2472, 2019.

Seneviratne, S. I., Nicholls, N., Easterling, D., Goodess, C. M., Kanae, S., Kossin, J., Luo, Y., Marengo, J., Mc Innes, K., Rahimi, M., et al.: Changes in climate extremes and their impacts on the natural physical environment, in: Managing the Risks of Extreme Events and Disasters to Advance Climate Change Adaptation: Special Report of the Intergovernmental Panel on Climate Change, pp. 109–230, Cambridge University Press, 2012.

Seneviratne, S. I., Zhang, X., Adnan, M., Badi, W., Dereczynski, C., Luca, A. D., Ghosh, S., Iskandar, I., Kossin, J., Lewis, S., et al.: Weather and climate extreme events in a changing climate, 2021.

Shah, J., Hari, V., Rakovec, O., Markonis, Y., Samaniego, L., Mishra, V., Hanel, M., Hinz, C., and Kumar, R.: Increasing footprint of climate warming on flash droughts occurrence in Europe, Environmental Research Letters, 17, 064 017, 2022.

Spinoni, J., Naumann, G., Vogt, J. V., and Barbosa, P.: The biggest drought events in Europe from 1950 to 2012, Journal of Hydrology: Regional Studies, 3, 509–524, 2015.

Spinoni, J., Naumann, G., Vogt, J., and Barbosa, P.: Meteorological droughts in Europe: events and impacts-past trends and future projections, Publications Office of the European Union, 2016.

Spinoni, J., Vogt, J. V., Naumann, G., Barbosa, P., and Dosio, A.: Will drought events become more frequent and severe in Europe?, International Journal of Climatology, 38, 1718–1736, 2018.

Spinoni, J., Barbosa, P., Bucchignani, E., Cassano, J., Cavazos, T., Christensen, J. H., Christensen, O. B., Coppola, E., Evans, J., Geyer, B., et al.: Future global meteorological drought hot spots: a study based on CORDEX data, Journal of Climate, 33, 3635–3661, 2020.

Stahl, K., Kohn, I., Blauhut, V., Urquijo, J., De Stefano, L., Acácio, V., Dias, S., Stagge, J. H., Tallaksen, L. M., Kampragou, E., et al.: Impacts of European drought events: insights from an international database of text-based reports, Natural Hazards and Earth System Sciences, 16, 801–819, 2016.

Staudinger, M., Stahl, K., and Seibert, J.: A drought index accounting for snow, Water Resources Research, 50, 7861–7872, 2014.

Tallaksen, L. M., Madsen, H., and Clausen, B.: On the definition and modelling of streamflow drought duration and deficit volume, Hydrological Sciences Journal, 42, 15–33, 1997.

https://doi.org/10.5194/egusphere-2026-973
Preprint. Discussion started: 4 March 2026

Teuling, A. J., Van Loon, A. F., Seneviratne, S. I., Lehner, I., Aubinet, M., Heinesch, B., Bernhofer, C., Grünwald, T., Prasse, H., and Spank, U.: Evapotranspiration amplifies European summer drought, Geophysical Research Letters, 40, 2071–2075, 2013.

Thakur, V., Markonis, Y., Kumar, R., Thomson, J. R., Vargas Godoy, M. R., Hanel, M., and Rakovec, O.: Unveiling the impact of potential evapotranspiration method selection on trends in hydrological cycle components across Europe, Hydrology and Earth System Sciences, 29, 4395–4416, 2025.

Van Loon, A. F.: Hydrological drought explained, Wiley Interdisciplinary Reviews: Water, 2, 359–392, 2015.

Van Loon, A. F. and Van Lanen, H. A.: A process-based typology of hydrological drought, Hydrology and Earth System Sciences, 16, 1915–1946, 2012.

Vautard, R., Gobiet, A., Sobolowski, S., Kjellström, E., Stegehuis, A., Watkiss, P., Mendlik, T., Landgren, O., Nikulin, G., Teichmann, C., et al.: The European climate under a 2 C global warming, Environmental Research Letters, 9, 034 006, 2014.

Xu, M., Hou, Z., Kang, S., Wu, X., Han, H., and Wang, P.: Projection of snowfall and precipitation phase changes over the Northwest China based on CMIP6 multimodels, Journal of Hydrology, 641, 131 743, 2024.

Yevjevich, V. M. et al.: An objective approach to definitions and investigations of continental hydrologic droughts, vol. 23, Colorado State University Fort Collins, CO, USA, 1967.

Zampieri, M., Ceglar, A., Dentener, F., and Toreti, A.: Wheat yield loss attributable to heat waves, drought and water excess at the global, national and subnational scales, Environmental Research Letters, 12, 064 008, 2017.